Stochastic modeling of transient boundary layers in high-Rayleigh-number thermal convection

Marten Klein[1]* · Heiko Schmidt[1] · Alan R. Kerstein[2]

Brandenburg University of Technology Cottbus - Senftenberg

[1]Numerical Fluid and Gas Dynamics, Brandenburg University of Technology (BTU), Cottbus, Germany *Contact: marten.klein@b-tu.de
[2]Consultant, Stochastic Science, Danville, CA, USA

Introduction

- **Turbulent thermal convection** denotes the chaotic flow in a layer of fluid that is driven by buoyancy forces due to an unstable temperature stratification. The flow becomes turbulent when buoyancy and inertial forces are much larger than viscous forces. This type of flow is encountered in numerous applications that range from technical to atmospheric and astrophysical scales (e.g. [1]).
- In a closed sample, **transient boundary layers** achieve the bulk-surface coupling (e.g. [2, 3]). These are mixed-type convective Blasius boundary layers (e.g. [4]) that control the achievable heat transfer (e.g. [5])

Main objectives

- Investigation of **transient boundary layers** in turbulent Rayleigh–Bénard convection.
- **Modeling** using a numerical tool applicable throughout the **relevant parameter space**.
- Capture **wall-normal transport processes** in mixed-type (Blasius-convective) boundary layers by utilizing a stochastic **one-dimensional turbulence** (ODT) model [6].

Model formulation

The **ODT model** aims to **resolve all relevant scales** of a turbulent flow along a notional line-of-sight ('ODT line'). Flow variables are resolved along this line on a dynamically adaptive grid [7]. Instantaneous flow profiles are evolved by **deterministic diffusion** along the ODT domain, and a **stochastic process** that models the effects of turbulent advection, pressure fluctuations, and buoyancy forces that are aligned with the ODT domain (z coordinate) [6, 8, 9].

- **ODT equations** for Cartesian velocity components $(u_i) = (u, v, w)$ and temperature T are [9]

$$\frac{\partial u_i}{\partial t} + \mathcal{E}_i(\alpha) = \nu \frac{\partial^2 u_i}{\partial z^2} \,, \qquad \frac{\partial T}{\partial t} + \mathcal{E}_T = \kappa \frac{\partial^2 T}{\partial z^2} \,,$$

  where ν is the kinematic viscosity and κ the thermal diffusivity.
- **Stochastic terms** $\mathcal{E}_i$ and $\mathcal{E}_T$ represent the effects of discrete turbulent **mapping ('eddy') events** in which the **triplet map** models the overturning motion of a turbulent eddy (**Fig. 1**).
- The **'eddy' rate** $\tau^{-1}(\ell, z_0; t)$ of a size-ℓ 'eddy' event at location z_0 at time t depends on the **local total available energy** for the momentary flow state. The eddy rate is [8, 9]

$$\tau^{-1} = C \sqrt{\frac{2}{\rho_0 V \ell^2} \left(E_\text{kin} - E_\text{pot} - Z\, E_\text{vp}\right)} \,,$$

  where ρ_0 is the reference mass density, $V = \ell^3$ the notional 'eddy' volume, E_kin and E_pot the local changes in the 'eddy' kinetic and potential energy, respectively, and E_vp is a viscous penalty energy that effectively suppresses unphysically small 'eddy' events below the viscous length scale [6].
- **Fixed ODT model parameters** $C = 60$, $Z = 220$, and $\alpha = 2/3$ are used here. Definitions are identical to [9], but we rely on the calibration performed in [10].

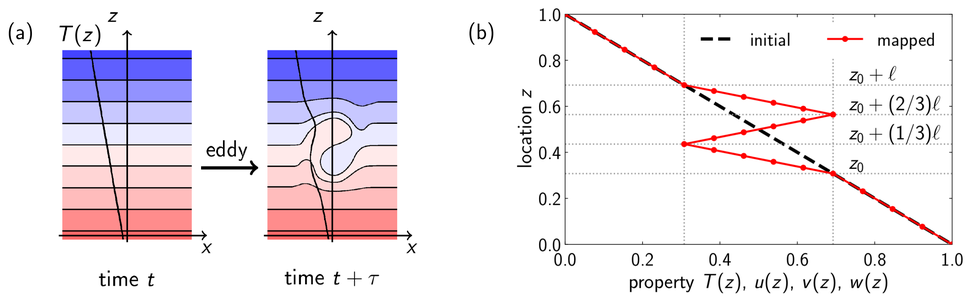

Figure 1: (a) Schematic of a notional 'eddy' turnover. (b) Triplet mapping in a turbulent 'eddy' event.

Flow configuration and model application

- **Layer of fluid** of height L for which wall-normal transport is resolved by a vertical ODT line as sketched in **Fig. 2(a)**
- **Transient boundary layers** form over the heated and cooled wall as sketched in **Fig. 2(b)**
- Uniform **constant gravity** $g = -g\, e_z$
- **Oberbeck–Boussinesq fluid:** linear equation of state, $\rho(T) = \rho_0[1 - \beta(T - T_0)]$, where β denotes the thermal expansion coefficient and the subscript '0' the reference values
- **Smooth constant-temperature no-slip wall:** heated wall (T_hw) at bottom $z = 0$ and cooled wall (T_cw) at top $z = L$ with prescribed constant temperature difference $\Delta T = T_\text{hw} - T_\text{cw}$
- The flow is characterized by the **Prandtl** (Pr) and **Rayleigh** (Ra) **number** that are fixed at

$$Pr = \frac{\nu}{\kappa} = 0.7 \qquad \text{and} \qquad Ra = \frac{g\,\beta\,\Delta T\,L^3}{\nu\kappa} = 3 \times 10^{10} \,.$$

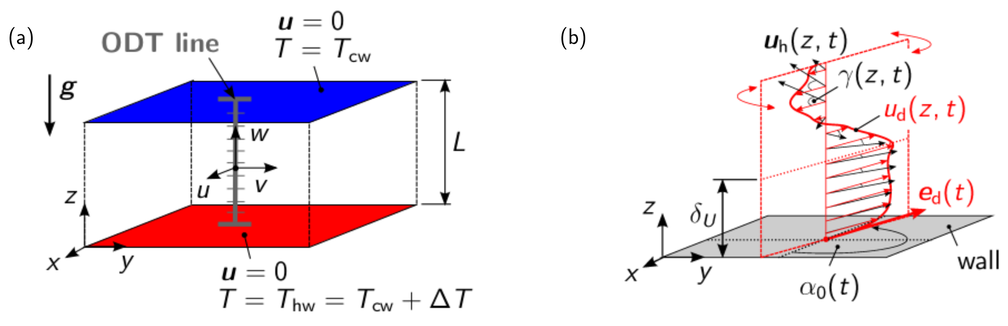

Figure 2: (a) Sketch of the canonical Rayleigh–Bénard set-up investigated. We focus on wall-normal transport far from the lateral walls (which are located at infinity) and resolve the flow only along a notional vertical 'ODT line'. (b) Sketch of the momentary local viscous boundary layer of thickness δ_U. Here $u_\text{h} = (u, v, 0)^\text{T}$ denotes the horizontal velocity vector, e_d the momentary boundary-layer 'downstream' direction, u_d the corresponding momentary 'downstream' velocity component, α_0 the momentary wall-shear angle, and γ the local deviation angle between u_h and e_d.

Transient boundary layers in thermal convection

- **Fig. 3(a)** shows the **normalized mean temperature**

$$\Theta(z) = \left(\langle T(z,t)\rangle - T_\text{b}\right)/\Delta T \qquad \text{with} \quad T_\text{b} = (T_\text{hw} + T_\text{cw})/2 \,,$$

  where T_b is the bulk temperature that is here measured at the midplane $z = L/2$. Angle brackets $\langle\cdot\rangle$ denote a conventional temporal average. **ODT captures** the **linear surface layer** and the **thermal log layer** (dashed green lines). The prefactor A in $\Theta(z) = A\,\ln(z/L) + B$ is obtained with ODT and the reference direct numerical simulation (DNS) [11], but not the additive constant B.
- **Fig. 3(b)** shows the **root-mean-square (r.m.s.) fluctuation temperature** σ_T, which is obtained for $\phi = T$ from the general formula

$$\sigma_\phi(z) = \sqrt{\langle\phi^2(z,t)\rangle - \langle\phi(z,t)\rangle^2} \,.$$

  ODT and DNS [11] results have been normalized by their maximum value σ_T^max. This maximum is nominally expected as monomodal peak at $z = \delta_T$ but ODT exhibits a bimodal peak due to missing fluctuations. This is a modeling artifact of the triplet map (**Fig. 1**) as shown in [7] for channel flow.
- **Fig. 3(c)** shows the **boundary-layer 'downstream' velocity** $\langle u_\text{d}\rangle$ that is obtained by conditional averaging of the momentary projected velocity $u_\text{d}(z,t)$, where

$$u_\text{d}(z,t) = e_\text{d}(t)\cdot u(z,t) \qquad \text{with} \qquad e_\text{d} = \left(\tau_{xz} e_x + \tau_{yz} e_y\right)/\tau_\text{w} \,, \qquad \tau_\text{w} = \sqrt{\tau_{xz}^2 + \tau_{yz}^2} \,,$$

  in which $\tau_{xz}(t)$ and $\tau_{yz}(t)$ are the horizontal (x, y) contributions to the momentary viscous wall-shear stress $\tau_\text{w}(t)$. $\langle u_\text{d}\rangle$ is compared with reference **horizontal r.m.s. fluctuation velocity** σ_U, where $U = \sqrt{u^2 + v^2}|_\text{axis}$ has been evaluated at the axis of a cylindrical sample [11]. In addition, **similarity functions** f_1 [12] and f_2 [13] for the streamwise r.m.s. fluctuation velocity σ_u from Blasius-type plate boundary layers (PBL) with matched $Re_\tau \approx 2180$ are shown. All data sets are normalized by their individual maximum value. ODT and reference data exhibit the *inner peak*. A small *log region* is seen in ODT and DNS [11] that would emerge in f_2 for larger Re_τ. The *outer peak* ('shoulder') is less pronounced in present ODT results which is consistent with the transient PBL studied in [14].
- **Fig. 3(d)** shows the **r.m.s. deviation angle** σ_γ for $\phi = \gamma$ denotes the local deviation angle,

$$\gamma(z,t) = \arctan\left(\frac{v(z,t)}{u(z,t)}\right) - \alpha_0(t) \,,$$

  which is measured between $u_\text{h} = (u, v, 0)^\text{T}$ and $e_\text{d} = (\cos\alpha_0, \sin\alpha_0, 0)^\text{T}$. The deviation angle is small for $z < \delta_U$ which supports the presence of a locally downstream-oriented Blasius-type surface layer.
- The thermal (δ_T) and viscous (δ_U) **boundary-layer thickness** have been obtained with the **slope method** (e.g. [11]) for Θ (**Fig. 3(a)**) and $\langle u_\text{d}\rangle$ (**Fig. 3(c)**), respectively. The shaded and hatched intervals give the **log-layer fitting ranges** used for ODT and DNS, respectively.

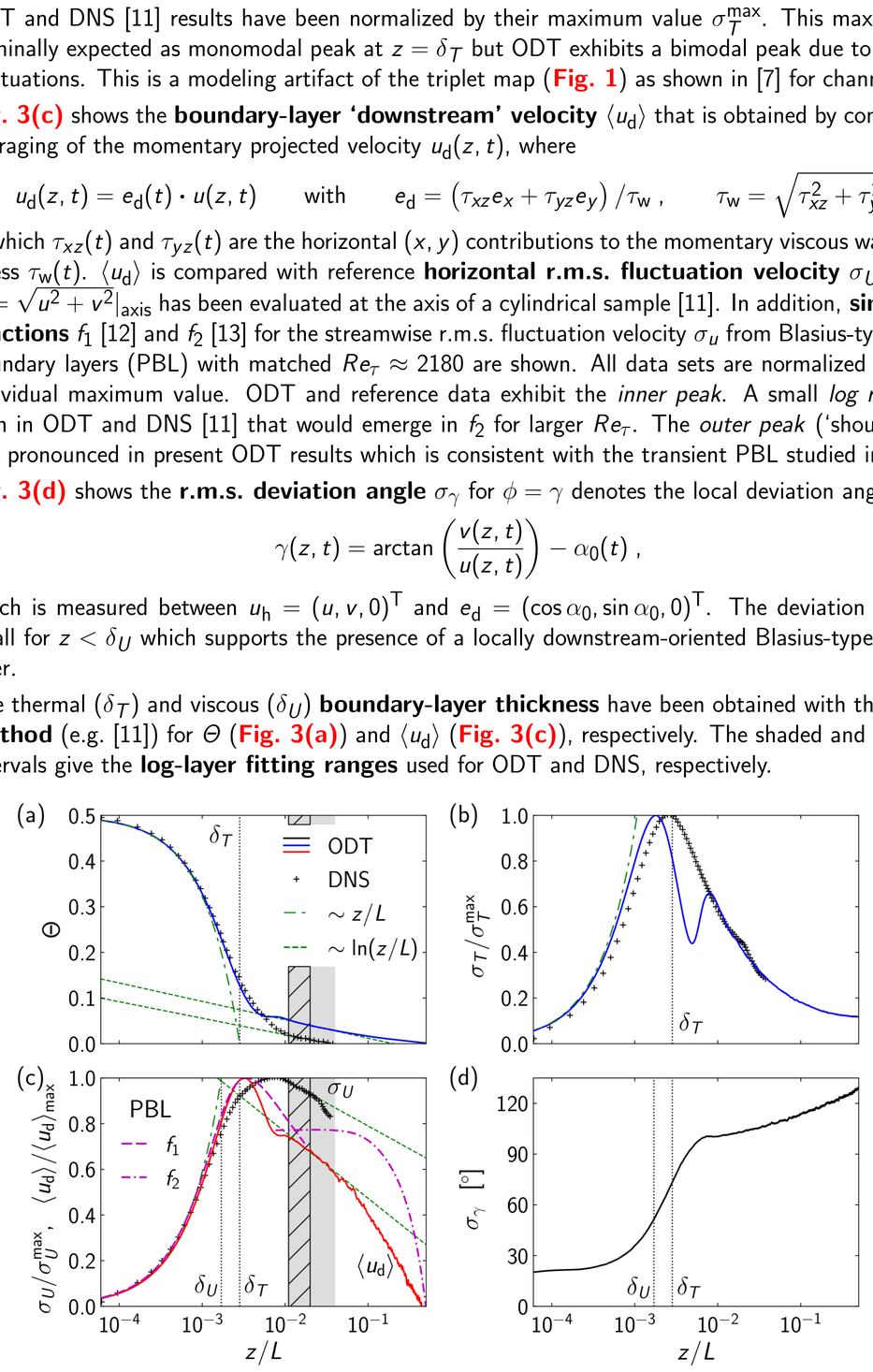

Figure 3: Thermal and viscous boundary-layer statistics in Rayleigh–Bénard convection for ODT and reference DNS [11]. (a) Normalized mean temperature Θ. (b) Root-mean-square (r.m.s.) fluctuation temperature σ_T. (c) Boundary-layer 'downstream' velocity $\langle u_\text{d}\rangle$ together with reference r.m.s. fluctuation velocity σ_U [11] and plate boundary-layer (PBL) r.m.s. similarity functions f_1 and f_2 [12, 13]. (d) ODT simulated r.m.s. deviation angle σ_γ. Thermal (δ_T) and viscous (δ_U) boundary-layer thicknesses are given for orientation. Log layers were fitted across shaded and hatched intervals.

Conclusions

- **ODT** is a dimensionally reduced, **stochastic turbulence model** that aims to resolve the wall-normal (vertical) transport processes on **all relevant scales** of the flow.
- ODT exhibits **transient convective Blasius boundary layers** over the heated and cooled wall capturing relevant surface-layer fluctuation statistics.
- Local 'downstream' velocity conditional statistics exhibit the *inner peak*, which is well described by **plate boundary-layer similarity functions** [12, 13] for matched Re_τ. The *outer peak* is weaker in ODT consistent with [14].

References

[1] F. Chillà, J. Schumacher, *Eur. Phys. J. E* **35**, 58 (2012).
[2] J. Schumacher, V. Bandaru, A. Pandey, J. D. Scheel, *Phys. Rev. Fluids* **1**, 084402 (2016).
[3] E. S. C. Ching, O.-Y. Dung, O. Shishkina, *J. Stat. Phys.* **167**, 626 (2017).
[4] N. Shi, M. S. Emran, J. Schumacher, *J. Fluid Mech.* **706**, 5 (2012).
[5] S. Grossmann, D. Lohse, *Phys. Fluids* **23**, 045108 (2011).
[6] A. R. Kerstein, *J. Fluid Mech.* **392**, 277 (1999).
[7] D. O. Lignell, A. R. Kerstein, G. Sun, E. I. Monson, *Theor. Comp. Fluid Dyn.* **27**, 273 (2013).
[8] S. Wunsch, A. R. Kerstein, *J. Fluid Mech.* **528**, 173 (2005).
[9] E. D. Gonzalez-Juez, A. R. Kerstein, D. O. Lignell, *Geophys. Astro. Fluid Dyn.* **107**, 506 (2013).
[10] M. Klein, H. Schmidt, *Proc. 11th Int. Symp. Turb. Shear Flow Phen.* (Southampton, UK, 2019), vol. 1, pp. 1–6.
[11] L. Li, *et al.*, *Phys. Rev. E* **86**, 026315 (2012).
[12] I. Marusic, A. K. M. Uddin, A. E. Perry, *Phys. Fluids* **9**, 3718 (1997).
[13] I. Marusic, G. J. Kunkel, *Phys. Fluids* **15**, 2461 (2003).
[14] Rakhi, M. Klein, J. A. Medina Méndez, H. Schmidt, *J. Turbul.* **20**, 506 (2019).